

where A_m and A_n are real quantities. After some transformations, we have from (12) and (23) the following two equations

$$\left. \begin{aligned} \beta_m \beta_n A_m A_n + k_d^2 = 0 \\ \beta_m^2 - \beta_n^2 + 2\omega\mu\nu(\beta_n A_n - \beta_m A_m) = 0 \end{aligned} \right\}. \quad (36)$$

These relations show the correlations between the polarization parameters and the propagation constants of two propagating modes.

IV. CONCLUSION

In this paper we have obtained two types of mode orthogonality in chirowaveguides. The first one is based on the vector equation of the eigenfunction problem. The vector formulated orthogonality (so-called power orthogonality) is a general form of orthogonality.

The second type of mode orthogonality is derived on the basis of scalar equations. We have obtained the scalar formulated orthogonality relations for two parallel-plate isotropic chirowaveguides. It is evident that this type of orthogonality differs from the vector formulated orthogonality for the same structure of chirowaveguide.

In this paper we have given special attention to a problem of complex modes in chirowaveguides. Active power flow in a waveguide may take place by combination of two complex modes of the spectrum. We have obtained the correlation between field components of two complex modes that transfer active power flow. The polarization of complex modes in chirowaveguides is different from the polarization of propagating and evanescent modes. According to our analysis, one can correlate the polarization parameters of modes with their propagation constants.

ACKNOWLEDGMENT

The author would like to thank Prof. A. Hardy for his attention to this paper and the stimulating debates they had in connection to it.

REFERENCES

- [1] P. Pelet and N. Engheta, "The theory of chirowaveguides," *IEEE Trans. Antennas Propagat.*, vol. 38, no. 1, pp. 90-98, 1990.
- [2] S. F. Mahmoud, "On mode bifurcation in chirowaveguides with perfect electric walls," *J. Electromagn. Waves Appl.*, vol. 6, no. 10, pp. 1381-1392, 1992.
- [3] H. Cory and S. Waxman, "Wave propagation along a fully or a partially loaded parallel plate chirowaveguide," *IEE Proc.*, pt. H, vol. 141, no. 4, pp. 299-306, 1994.
- [4] H. Cory and I. Rosenhouse, "Electromagnetic wave propagation along a chiral slab," *IEE Proc.*, pt. H, vol. 138, no. 1, pp. 51-54, 1991.
- [5] M. I. Oksanen, P. K. Koivisto, and I. V. Lindell, "Dispersion curves and fields for a chiral slab waveguide," *IEE Proc.*, pt. H, vol. 138, no. 4, pp. 327-334, 1991.
- [6] C. Eftimiu and L. W. Pearson, "Guided electromagnetic waves in chiral media," *Radio Sci.*, vol. 24, no. 3, pp. 351-359, 1989.
- [7] G. Busse and A. F. Jacob, "Complex modes in circular chirowaveguides," *Electron. Lett.*, vol. 29, no. 8, pp. 711-713, 1993.
- [8] P. Pelet and N. Engheta, "Modal analysis for rectangular chirowaveguides with metallic walls using the finite-difference method," *J. Electromagn. Waves Appl.*, vol. 6, no. 9, pp. 1277-1285, 1992.
- [9] H. Cory, "Wave propagation along a closed rectangular chirowaveguide," *Microwave Opt. Technol. Lett.*, vol. 6, no. 14, pp. 797-800, 1993.
- [10] N. Engheta and P. Pelet, "Surface waves in chiral layers," *Opt. Lett.*, vol. 16, no. 10, pp. 723-725, 1991.
- [11] N. Engheta, D. L. Jaggard, and M. W. Kowarz, "Electromagnetic waves in Faraday chiral media," *IEEE Trans. Antennas Propagat.*, vol. 40, no. 4, pp. 367-374, 1992.
- [12] Z. Shen, "The theory of chiroferrite waveguides," *Microwave Opt. Technol. Lett.*, vol. 6, no. 7, pp. 397-401, 1993.
- [13] N. Engheta and P. Pelet, "Mode orthogonality in chirowaveguides," *IEEE Trans. Microwave Theory Tech.*, vol. 38, no. 11, pp. 1631-1634, 1990.
- [14] L. B. Felsen and N. Marcuvitz, *Radiation and Scattering of Waves*. Englewood Cliffs, NJ: Prentice-Hall, 1973, ch. 1.
- [15] E. O. Kamenetskii, "Spectral method for modes excitation problem in anisotropic waveguides," *IEEE Trans. Microwave Theory Tech.*, vol. 42, no. 9, pp. 1685-1689, 1994.
- [16] A. S. Omar and K. F. Schünemann, "Complex and backward-wave modes in inhomogeneously and anisotropically filled waveguides," *IEEE Trans. Microwave Theory Tech.*, vol. MTT-35, no. 3, pp. 268-275, 1987.
- [17] G. L. Veselov and S. V. Raelevskiy, *The Layered Metallic Dielectric Waveguides*. Moscow: Radio i svyaz, 1988 (in Russian).
- [18] R. Marques, F. L. Mesa, and M. Horro, "Nonreciprocal and reciprocal complex and backward waves in parallel plate waveguides loaded with a ferrite slab arbitrarily magnetized," *IEEE Trans. Microwave Theory and Tech.*, vol. 41, no. 8, pp. 1409-1418, 1993.
- [19] F. Mariotte and N. Engheta, "Reflection and transmission of guided electromagnetic waves at an air-chiral interface and at a chiral slab in a parallel-plate waveguide," *IEEE Trans. Microwave Theory Tech.*, vol. 41, no. 11, pp. 1895-1906, 1993.

Development of Semi-Empirical Design Equations for Symmetrical Three-Line Microstrip Couplers

Lukang Yu and Banmali Rawat

Abstract—Semi-empirical design equations for symmetrical three-line microstrip couplers (TMC's) have been developed. The approach is based on dividing the total capacitance of the system into various basic capacitances, which are then calculated empirically and semi-numerically. The numerical results based on these design equations have been found in good agreement with the previously obtained results.

I. INTRODUCTION

Symmetrical TMC's have been investigated by many authors [1]–[6]. The quasi-static characteristics of these couplers can be completely determined from the capacitance matrix of the structure. For design purposes, a table or a graph for many sets of line parameters has to be prepared. Various methods for calculating the static capacitances inevitably involve time-consuming numerical procedures. This paper intends to derive closed-form expressions for the characteristics of symmetrical TMC's. The approach is based on the division of the total capacitance of the structure into various basic capacitances. These basic capacitances can then be calculated empirically and semi-numerically.

II. DIVISION OF THE TOTAL CAPACITANCE

The division of the total capacitance of a symmetrical TMC into parallel-plate, fringe, and gap capacitances is shown in Fig. 1. The three propagation modes of the coupler are designated as *A*-, *B*-, and *C*-modes, which correspond to *ee*-, *oo*-, and *oe*-modes, respectively, in [6]. Due to the symmetrical configuration, the vertical centerline of the cross section is replaced by a magnetic wall for *A*- and *B*-modes, or an electric wall for *C*-mode. Using Fig. 1(a), the effective dielectric

Manuscript received January 9, 1995; revised November 27, 1995.

The authors are with the Department of Electrical Engineering, University of Nevada, Reno, NV 89557 USA.

Publisher Item Identifier S 0018-9480(96)01560-8.

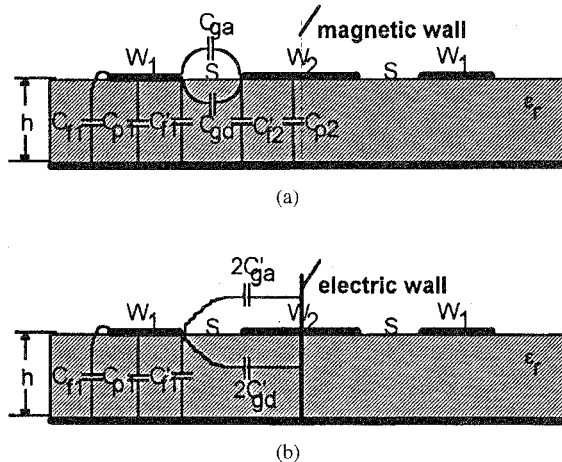


Fig. 1. (a) Static capacitances for *A*- and *B*-mode and (b) static capacitances for *C*-mode.

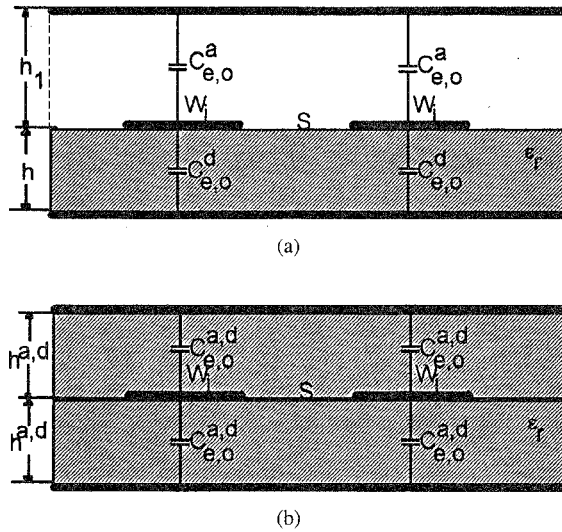


Fig. 2. (a) Symmetrical coupled microstrips with ground cover. (b) Symmetrical coupled striplines.

constants and characteristic impedances of *A*- and *B*-modes can be calculated from the self and mutual capacitances and inductances of two asymmetric lines as [7]

$$\varepsilon_{A,B} = 2v_0^2 [L_{11}C_{11} + L_{22}C_{22} - 2L_{12}C_{12} \pm \Sigma]^{-1} \quad (1)$$

$$Z_{A1,B1} = \frac{v_0}{\sqrt{\varepsilon_{A,B}}} \left[L_{11} - \frac{L_{12}}{R_{A,B}} \right] \quad (2)$$

$$Z_{A2,B2} = \frac{-R_A R_B}{2} Z_{A1,A2} \quad (3)$$

where

$$R_{A,B} = \frac{(L_{11}C_{11} - L_{22}C_{22}) \pm \Sigma}{2(L_{12}C_{11} - L_{22}C_{12})} \quad (4)$$

and as in (5), shown at the bottom of the page, and v_0 is the velocity of light in free space.

The self and mutual capacitances C_{11} , C_{22} , and C_{12} may be written in terms of the parallel-plate, fringe, and gap capacitances, using Fig.

1(a) as follows:

$$C_{11} = C_{p1} + C_{f1} + C'_{f1} + C_{gd} + C_{ga} \quad (6)$$

$$C_{22} = 0.5C_{p2} + C'_{f2} + C_{gd} + C_{ga} \quad (7)$$

$$C_{12} = C_{gd} + C_{ga} \quad (8)$$

where C_{p1} is the parallel plate capacitance between side strip (W_1) and the ground plane; C_{f1} is the outside fringe capacitance between side strip (W_1) and the ground plane; C'_{f1} is the inside fringe capacitance between side strip (W_1) and the ground plane; C_{gd} is the gap capacitance through dielectric between the side strip (W_1) and center strip (W_2); C_{ga} is the gap capacitance through air between the side strip (W_1) and center strip (W_2); C'_{f2} is the fringe capacitance between center strip (W_2) and the ground plane; and C_{p2} is the parallel plate capacitance between the center strip (W_2) and the ground plane.

The self and mutual inductances L_{11} , L_{22} , and L_{12} are determined using $[L] = [C^a]^{-1} / v_0^2$ where C^a 's are self and mutual capacitances when the dielectric is replaced by air. The characteristics of *C*-mode are given as

$$\varepsilon_C = \frac{C_C}{C_C^a} \quad (9)$$

$$Z_C = \frac{1}{v_0 \sqrt{C_C C_C^a}} \quad (10)$$

where C_C^a is the *C*-mode capacitance with air as dielectric, and using Fig. 1(b)

$$C_C = C_{p1} + C_{f1} + C'_{f1} + 2(C'_{gd} + C'_{ga}) \quad (11)$$

where C_{p1} , C_{f1} , and C'_{f1} are the capacitances as defined before but for *C*-mode. C'_{gd} and C'_{ga} are the capacitances between the side strips through dielectric and air, respectively.

III. CALCULATION OF BASIC CAPACITANCES

The basic capacitances are calculated by using the expressions derived for single and coupled microstrips. The parallel-plate capacitances are given by

$$C_{pi} = \varepsilon_0 \varepsilon_r \frac{W_i}{h} \quad i = 1, 2 \quad (12)$$

while the outside fringe capacitances are calculated from the total capacitance of the single microstrip as

$$C_{fi} = 0.5 \left(\frac{\varepsilon_i}{v_0 Z_{0mi}} - C_{pi} \right) \quad i = 1, 2 \quad (13)$$

where from [8]

$$Z_{0mi} = \begin{cases} 60 \ln [8h/W_i + W_i/4h], & W_i/h \leq 1 \\ 120\pi/[W_i/h + 1.393 + 0.677 \ln (W_i/h + 1.444)] & W_i/h \geq 1 \end{cases} \quad (14)$$

and as in (15), shown at the bottom of the next page.

The expressions for remaining capacitances are given by [9]

$$C'_{fi} = C_{ei} - C_{pi} - C_{fi} \quad i = 1, 2 \quad (16)$$

$$C_{gd} + C_{ga} = 0.5 \sqrt{[(C_{o1} - C_{e1})(C_{o2} - C_{e2})]} \quad (17)$$

$$C'_{gd} + C'_{ga} = 0.5(C'_o - C'_e) \quad (18)$$

$$\Sigma = \sqrt{[4(L_{12}C_{11} - L_{11}C_{12})(L_{12}C_{22} - L_{22}C_{12}) + (L_{11}C_{11} - L_{22}C_{22})^2]} \quad (5)$$

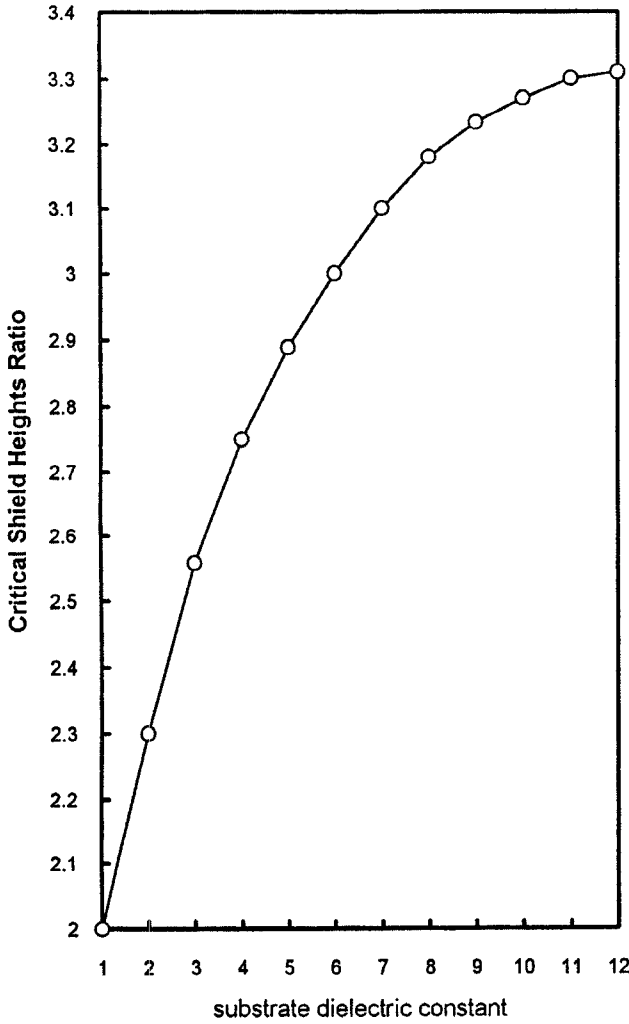
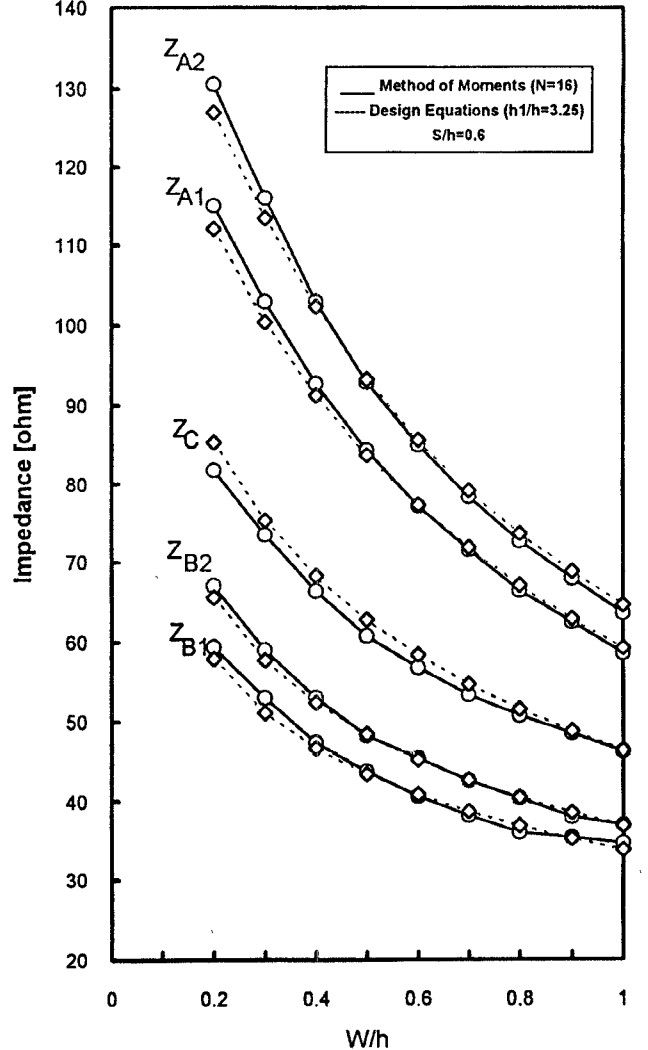


Fig. 3. Variation of critical heights ratio with dielectric constant.

where $C_{ei,oi}$ represents the even- or odd-mode capacitance of two symmetrical microstrips with strip width W_i ($i = 1, 2$) and spacing S . $C'_{eo,oi}$ represents the even- or odd-mode capacitance of two symmetrical microstrips with strip width W_1 and spacing $2S$. It is to be noted that $(C'_{eo,oi} + C'_{go,oi})$ accounts for the total capacitance between two symmetrical side microstrips for C -mode with spacing $2S$. In this case, the width of the center line is excluded from the spacing between the side lines due to the electric wall. This may introduce negligible error as the strip width is very small and the electric field lines terminate on the edges of the strip.

IV. EVEN- AND ODD-MODE CAPACITANCES OF COUPLED MICROSTRIPS

For more practical analysis, the coupled microstrip geometry with the ground cover as shown in Fig. 2(a) has been considered. The introduction of ground cover by no means affects the configurations discussed in previous sections as the ground cover height is more than the critical value to have any impact on field analysis. The total capacitance is broken up into air and dielectric capacitances. The total

Fig. 4. Comparison of mode impedances for design equations ($\epsilon_r = 9.8$).

even- and odd-mode capacitances may be written as

$$C_{ei,oi} = C_{eo,oi}^a + C_{eo,oi}^d \quad (19)$$

where $C_{eo,oi}^a$ represents the even- or odd-mode capacitance in the air region. It is taken as half the total-mode capacitance of the corresponding coupled striplines with the same values of S and W_i as for the shielded microstrips and with the dielectric thickness being $2h_1$ and containing air as dielectric, as shown in Fig. 2(b). $C_{eo,oi}^d$ represents the even- or odd-mode capacitance in the dielectric region. It is calculated as in the case of $C_{eo,oi}^a$ but with the dielectric thickness of the corresponding striplines being $2h$ and containing a dielectric material. These mode capacitances of the coupled striplines are calculated by conformal mapping as

$$C_{ei,oi}^{a,d} = 2\epsilon_0 \epsilon_r^{a,d} \frac{K(k_{ei,oi}^{a,d})}{K'(k_{ei,oi}^{a,d})} \quad (20)$$

$$\epsilon_i = \begin{cases} 0.5(\epsilon_r + 1) + 0.5(\epsilon_r - 1)(1 + 12h/W_i)^{-1/2} + 0.04(1 - W_i/h)^2, & W_i/h \leq 1 \\ 0.5(\epsilon_r + 1) + 0.5(\epsilon_r - 1)(1 + 12h/W_i)^{-1/2}, & W_i/h \geq 1 \end{cases} \quad (15)$$

TABLE I
COMPARISON OF MODE IMPEDANCES FOR $\varepsilon_r = 9.8$

W/h	S/h	Design Equations ($h_c/h=3.25$)						The Method of Moments (N=16)					
		Z _{A1}	Z _{A2}	Z _{B1}	Z _{B2}	Z _C	Z _{A1}	Z _{A2}	Z _{B1}	Z _{B2}	Z _C		
0.8	0.4	70.22	80.15	32.03	36.56	47.61	70.88	80.56	30.52	35.69	46.26		
0.614	0.309	82.41	98.78	31.42	37.66	49.86	83.28	99.78	30.04	35.99	49.59		
0.5	0.2	93.45	121.9	27.60	36.01	47.79	95.44	123.0	26.60	35.28	49.54		
0.4	0.15	103.4	147.7	25.23	36.03	48.47	107.9	147.1	25.06	35.18	50.35		

where $K(k_{\text{even}}^{a,d})$ and $K'(k_{\text{even}}^{a,d})$ are the elliptical function and its complement with

$$k_{\text{even}}^{a,d} = \begin{cases} \tanh\left(\frac{\pi W_i}{4h^{a,d}}\right) / \tanh\left(\frac{\pi(W_i + S)}{4h^{a,d}}\right) & \text{for odd-mode} \\ \tanh\left(\frac{\pi W_i}{4h^{a,d}}\right) \tanh\left(\frac{\pi(W_i + S)}{4h^{a,d}}\right) & \text{for even-mode} \end{cases} \quad (21)$$

In the above equations, $h^a = h_1, h^d = h, \varepsilon_r^a = 1, \varepsilon_r^d = \varepsilon_r$, and $i = 1, 2$.

Similarly, C_{even}^a and C_{even}^d as given in (18) for C -mode are determined by using the corresponding coupled stripline structures and are given as

$$C_{\text{even}}^a = C_{\text{even}}^{a,d} + C_{\text{even}}^{d,d} \quad (22)$$

where $C_{\text{even}}^{a,d}$ is calculated using (20), but $k_{\text{even}}^{a,d}$ with being

$$k_{\text{even}}^{a,d} = \begin{cases} \tanh\left(\frac{\pi W}{4h^{a,d}}\right) / \tanh\left(\frac{\pi(W_1 + 2S)}{4h^{a,d}}\right) & \text{for odd-mode} \\ \tanh\left(\frac{\pi W_1}{4h^{a,d}}\right) \tanh\left(\frac{\pi(W_1 + 2S)}{4h^{a,d}}\right) & \text{for even-mode} \end{cases} \quad (23)$$

Accurate and simple expressions for the ratio $K(k)/K'(k)$ are available and given below for $k'^2 = 1 - k^2$

$$\frac{K(k)}{K'(k)} = \begin{cases} \frac{1}{\pi} \ln\left(2 \frac{1 + \sqrt{k}}{1 - \sqrt{k}}\right) & \text{for } 0.5 \leq k^2 \leq 1 \\ \frac{1}{\pi} \ln\left(2 \frac{1 + \sqrt{k'}}{1 - \sqrt{k'}}\right) & \text{for } 0 \leq k^2 \leq 0.5 \end{cases} \quad (24)$$

V. NUMERICAL RESULTS AND DISCUSSION

In order to apply the design equations for the cases of three coupled microstrips, the critical heights ratio h_{c1}/h is used. The critical height h_{c1} is the lower bound of the ground cover height, necessary to obtain sufficiently accurate results. It is calculated by comparing the results of the mode impedances of three coupled microstrips to those obtained in [6] and defining h_{c1}/h as that ratio for which the two results are in agreement to within 5% h_{c1}/h as a function of the substrate dielectric constant is shown in Fig. 3.

The calculated mode impedances for $\varepsilon_r = 9.8$ are compared with the results obtained by using the method of moments [6], as shown in Table I, with N as the number of substrips. The values of mode impedances obtained by using the design equations have an error less than 5% for the parameters lying in the range $\varepsilon_r \geq 1, 0.1 \leq W_i/h \leq 1$ and $0.1 \leq S/h \leq 1$. The programs were run on a 386 IBM-PC. The computational time for obtaining these values is less than one second as compared to 10 min when the method of moments is used.

The mode impedances for $S/h = 0.6, \varepsilon_r = 9.8$ and various W/h ratios are plotted in Fig. 4.

VI. CONCLUSION

The derivation of semi-empirical design equations facilitates the design of symmetrical TMC's in terms of the faster generation of design curves with error less than the fabrication tolerance. If ε_{eq} and h_{eq} are substituted for ε_r and h , the characteristics of anisotropic TMC's are calculated. It should be pointed that in these design equations, the finite strip-thickness has not been considered.

REFERENCES

- [1] D. Pavlidis and H. L. Hartnagel, "The design and performance of three-line microstrip couplers," *IEEE Trans. Microwave Theory Tech.*, vol. MTT-24, pp. 631-640, Oct. 1976.
- [2] V. K. Tripathi, "On the analysis of symmetrical three-line microstrip circuits," *IEEE Trans. Microwave Theory Tech.*, vol. MTT-25, pp. 726-729, Sept. 1977.
- [3] —, "The scattering parameters and directional coupler analysis of characteristically terminated three-line structures in an inhomogeneous medium," *IEEE Trans. Microwave Theory Tech.*, vol. MTT-29, pp. 22-26, Jan. 1981.
- [4] E. A. F. Abdallah and N. A. El-Deeb, "On the analysis and design of three coupled microstrip lines," *IEEE Trans. Microwave Theory Tech.*, vol. MTT-33, pp. 1217-1222, Nov. 1985.
- [5] N. A. El-Deeb, "An improved design of systems based on three coupled microstrip lines," *IEEE Trans. Microwave Theory Tech.*, vol. 37, pp. 795-798, Apr. 1989.
- [6] L. Yu and B. Rawat, "Quasi-static analysis of three-line microstrip symmetrical coupler on anisotropic substrates," *IEEE Trans. Microwave Theory Tech.*, vol. 39, pp. 1433-1437, Aug. 1991.
- [7] K. C. Gupta, R. Garg, and I. J. Bahl, *Microstrip Lines and Slotlines*. New York: Artech, 1979.
- [8] E. O. Hammerstad, "Equations for microstrip circuit design," in *5th Eur. Microwave Conf.*, 1975, pp. 268-272.
- [9] S. S. Bedair, "Characteristics of some asymmetrical coupled transmission lines," *IEEE Trans. Microwave Theory Tech.*, vol. MTT-32, pp. 108-110, Jan. 1984.